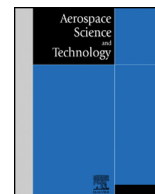




Contents lists available at ScienceDirect

## Aerospace Science and Technology

[www.elsevier.com/locate/aescte](http://www.elsevier.com/locate/aescte)

## Short communication

## An improved propeller design method for the electric aircraft

Song Xiang<sup>a,b</sup>, Yuan-qiang Liu<sup>b</sup>, Gang Tong<sup>a</sup>, Wei-ping Zhao<sup>a</sup>, Sheng-xi Tong<sup>b</sup>,  
Ya-dong Li<sup>b</sup><sup>a</sup> Liaoning Key Laboratory of General Aviation, Shenyang Aerospace University, No. 37 Daoyi South Avenue, Shenyang, Liaoning 110136, People's Republic of China<sup>b</sup> Liaoning General Aviation Academy, No. 37 Daoyi South Avenue, Shenyang, Liaoning 110136, People's Republic of China

## ARTICLE INFO

## Article history:

Received 5 January 2018

Received in revised form 2 May 2018

Accepted 7 May 2018

Available online xxxx

## Keywords:

Electric aircraft

High efficiency

Propeller

Wind tunnel test

New energy

## ABSTRACT

In this paper, an improved propeller design method for the electric aircraft was presented. For a given operative condition and profile distribution along the blade, the present method can determine the chord and pitch angle distribution of the blade, together with its efficiency and its torque and thrust coefficients of the maximum efficiency propeller. According to the flight velocity, thrust and rotate speed of cruise condition, the propeller of an electric aircraft was designed using the present method. Wind tunnel test of scaled model of propeller (diameter 0.96 m) was carried out. The test results show that present method was suitable to design the propeller of the electric aircraft.

© 2018 Published by Elsevier Masson SAS.

## 0. Introduction

Due to their 'near zero emission', low noise, electric aircraft powered by Lithium-ion battery are becoming increasingly attractive. In the world, several companies have researched and manufactured the electric aircraft powered by Lithium-ion batteries or fuel cells. For examples, Pipistrel company of Slovenia, Airbus company, Yuneec company of China, Shenyang Aerospace University of China.

Taurus Electro G2 of Pipistrel is the electric 2-seat aircraft in serial production available on the market. The propulsion motor of G2 weighs an impressive 11 kg (rather than 16 kg) and generates 40 kW power. Pipistrel's Taurus G4 [1] is the World's first four-seat electric aircraft with the unique twin-fuselage configuration, maximum take-off Weight of 1,500 kg, total energy capacity of 90 kWh, maximum power of 150 kW. G4 is the winner of the NASA Green Flight Challenge 2011, sponsored by Google. The E-Fan is a two-seater electric aircraft being developed by Airbus Group. The aircraft uses on-board lithium batteries to power the two electric motors and can carry two passengers. A test flight was conducted in April 2014 at Mérignac Airport, France. The target market is pilot training. Airbus announced that the E-Fan 2.0 will go into production by 2017 with a side-by-side seating layout. The Yuneec International E430 is a Chinese two-seat electric aircraft designed for commercial production by Yuneec. The first flight of the E430 took place from the Yuneec factory near Shanghai, China

on June 12, 2009. The RX1E is an electric powered two-seat, composite construction aircraft with a T-tail and tricycle landing gear. The aircraft was developed by the Shenyang Aerospace University, and is one of the first electric airplanes in production. The company has 28 orders for the aircraft. Politecnico di Torino [2–5] developed the environmentally friendly inter-city aircraft powered by fuel cells. The fuel cell system of ENFICA-FC was installed on the light RAPID 200 sports.

The propeller was used to generate thrust for the electric aircraft powered by Lithium-ion batteries or fuel cells. But the most of the existing propellers were designed for the conventional fuel engines. The fuel engine has sufficient torque to drive the propeller. Due to the torque of electric motor is limited, the design of the propeller for the electric aircraft is difficult. In order to enhance the endurance of the electric aircraft, a highly efficient propeller was required.

Many scholars have researched the design, analysis and testing of the propeller. Angelo et al. [6] presented two numerical procedures for the propeller. The first algorithm allows for the determination of the geometric characteristics of the maximum efficiency propeller for a given operative condition. The second algorithm allows for the evaluation of the efficiency, the thrust and torque coefficients of a propeller of known geometry. Romeo et al. [7] dealt with the design and testing of a propeller for a two-seater aircraft powered by fuel cells. In their studies, an optimal two-blade propeller has been designed and manufactured to be installed on the Rapid 200 FC airplane. Slavík [8] presented a method for preliminary determination of propeller thrust and power coefficients by

E-mail address: [xs74342@sina.com](mailto:xs74342@sina.com) (S. Xiang).

<https://doi.org/10.1016/j.ast.2018.05.008>

1270-9638/© 2018 Published by Elsevier Masson SAS.

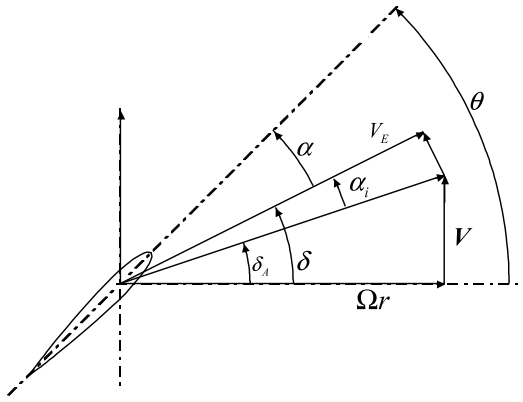


Fig. 1. Blade profile of radial position  $r$ .

means of blade chord and blade angle setting at 70% of the top radius, airfoil thickness at the radius near the tip and the position of the maximum blade width. Sabzehparvar [9] developed a propeller model that will accurately predict airplane engine static and dynamic thrust and torque in a full range of advance ratio. Morgado [10] presented the design and optimization of a propeller for on the MAAT cruiser airship by means of the inverse design methodology. Lieser et al. [11] performed the aeroacoustic calculation of a 6-bladed propeller by the blade element method. Rizk and Jouj [12] investigated and demonstrated the feasibility of combining an analysis code and an optimization procedure for designing propellers. Dorfling and Rokhsaz [13] presented a procedure for deriving the Euler-Lagrange equations for both unconstrained and constrained propeller blade-twist optimization. Chang and Sullivan [14] presented a method for the optimization of propeller twist. In their method, the propeller is represented by a curved lifting line and a number of control points. Chen et al. [15] experimentally studied the aerodynamic performance of the high-altitude propeller, especially the counter rotation effects. Influences of different configurations on a stratospheric airship, included 2-blade counter-rotating propeller (CRP), dual 2-blade single rotation propellers (SRPs) and 4-blade SRP, are also indicated. Their research indicates that the effect of counter rotation can greatly improve the efficiency.

In this paper, an improved propeller design method for the electric aircraft was presented. For a given operative condition and profile distribution along the blade, the present method can determine the chord and pitch angle distribution of the blade, together with its efficiency and its torque and thrust coefficients of the maximum efficiency propeller. According to the flight velocity, thrust and rotate speed of cruise condition, the propeller of an electric aircraft was designed using the present method. Wind tunnel test of scaled model of propeller was carried out.

## 1. Designed method of propeller

For a given thrust  $T$ , flight velocity  $V$ , rotation angular velocity of propeller  $\Omega$ , blade number  $n$ , propeller radius  $R$ , hub radius  $R_h$ , airfoil distribution along the blade, the energy loss of maximum efficiency propeller is minimum. If all the profile along the blade operates at the maximum efficiency (maximum lift to drag ratio), the propeller efficiency is maximum. Blade profile of radial position  $r$  is shown in Fig. 1.

Design procedure of the propeller with high efficiency is as follows:

(1) If the blade is divided into  $n_b$  sections ( $n_b + 1$  profiles)

(2) Determining the Lagrange multiplier  $K$ , the integral equation is as follows:

$$\frac{T}{\rho 4\pi V^2} = \int_{R-R_h}^R (K_1 + K_1^2) k_P r dr \quad (1)$$

where  $\rho$  is air density,  $k_P$  is correction factor.

$$k_P = \frac{2}{\pi} \arccos(e^{-\frac{\eta}{2}(1-\frac{r}{R})} \sqrt{1+(\frac{\Omega R}{V})^2}) \quad (2)$$

$$K_1 = \frac{K}{1+(\frac{V}{\Omega r})^2(1+K)^2} \quad (3)$$

In Angelo et al. [6], the each blade section chord is obtained by the iteration method. But in the present paper, the chord distribution along the blade can be determined by the following function:

$$b = c_1 \beta^{-(\xi_i - m)^2} \quad (4)$$

where non-dimensional chord length  $b = l/R$ ,  $l$  is the chord length of a profile,  $c_1$  is the maximum chord length among all profiles, non-dimensional radial coordinate of  $i$ th profile  $\xi_i = \frac{r_i}{R}$ ,  $m$  denotes the non-dimensional radial coordinate of a profile with maximum chord length,  $\beta$  is the chord distribution coefficient,  $2 \leq \beta \leq 100$ .

(3) Determining the pitch angle  $\theta$  of the  $i$ th profile.

The  $\delta$  is calculated by the Eq. (5).

$$\delta = \arctan \left[ \frac{\lambda}{\xi_i} (1 + K) \right] \quad (5)$$

where  $\lambda = \frac{V}{\Omega R}$  is the advanced ratio.

Induced attack angle  $\alpha_i$  can be calculated by the Eq. (6).

$$\alpha_i = \arctan \left( \frac{K \sin \delta \cos \delta}{1 + K \cos^2 \delta} \right) \quad (6)$$

$\hat{V}_E$  can be calculated by Eq. (7).

$$\hat{V}_E = \sqrt{1 + \left( \frac{\xi_i}{\lambda} \right)^2} \cos \alpha_i \quad (7)$$

Local Renold number and Mach number can be calculated by the Eq. (8).

$$Re_{\xi} = \hat{V}_E b \cdot Re, \quad Ma_{\xi} = \hat{V}_E \cdot Ma \quad (8)$$

where  $b$  can be obtained by the Eq. (4),  $Re$  is the Renold number of free stream,  $Re = \rho V R / \mu$ ,  $Ma$  is the Mach number of free stream,  $Ma = V/c$ ,  $c$  is the sound speed.

Xfoil6.96 is used to calculate the lift to drag ratio of airfoil.  $\alpha_{max}$  is the attack angle at maximum lift to drag ratio.  $Cl_{max}$  is the lift coefficient at attack angle  $\alpha_{max}$ .  $Cd_{max}$  is the drag coefficient at attack angle  $\alpha_{max}$ .

Pitch angle  $\theta$  of  $i$ th profile is

$$\theta = \delta + \alpha_{max} \quad (9)$$

(4) Repeating the Eqs. (5)–(9), we can obtain the pitch angle  $\theta$ , attack angle  $\alpha_{max}$ , lift coefficient  $Cl_{max}$  and drag coefficient  $Cd_{max}$  of each profile.

(5) Determining the efficiency of propeller

Thrust coefficient and torque coefficient can be calculated by Eq. (10) and Eq. (11), respectively.

$$\tau = \int_{\xi_{min}}^1 \frac{n\lambda^2}{2} \hat{V}_E^2 (Cl_{max} \cos \delta - Cd_{max} \sin \delta) b d\xi \quad (10)$$

$$\chi = \int_{\xi_{min}}^1 \frac{n\lambda^2}{2} \hat{V}_E^2 (Cl_{max} \sin \delta + Cd_{max} \cos \delta) b \xi d\xi \quad (11)$$



Fig. 2. RAF 6 airfoil.

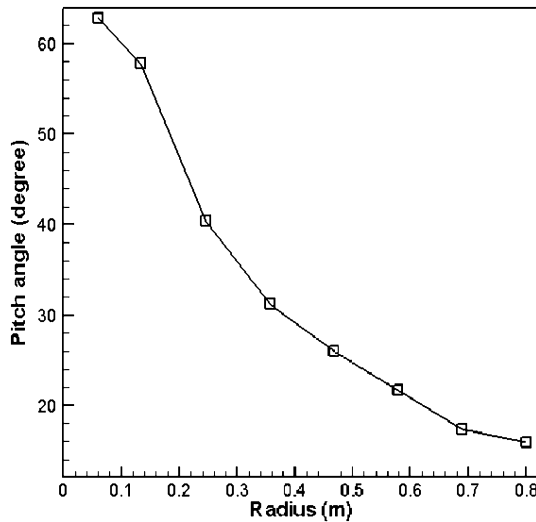


Fig. 3. Pitch angle distribution along the radial direction.

Efficiency of propeller is calculated by Eq. (12).

$$\eta = \frac{\tau \lambda}{X} \quad (12)$$

## 2. Design of a propeller for an electric aircraft

The electric aircraft is powered by Lithium-ion battery with the two-seater configuration, maximum take-off Weight of 500 kg, total energy capacity of 8.8 kWh, maximum power of 40 kW. According to the general design requirement, a two-blade fixed pitch wooden propeller is used to generate the thrust. The radius of propeller  $R = 0.8$  m, the radius of hub  $R_h = 0.06$  m, the blade is divided into 7 sections (8 profiles). RAF 6 airfoil is adopted as shown in Fig. 2.

The propeller is designed using the parameters of cruise condition. Flight velocity  $V = 100$  km/h, rotation speed 1600 (r/min), thrust  $T = 245$  N,  $c_1 = 0.1875$ ,  $\beta = 100$ ,  $m = \xi_3$ .

According to the above propeller design method, a propeller for an electric aircraft is designed. The chord and pitch angle distribution of the blade are obtained.

The pitch angle distribution along the radial direction is shown in Fig. 3.

It can be found from the Fig. 3 that pitch angle decreases gradually from the blade root to blade tip. Pitch angle at the blade root is 62.79 degree, at the blade tip is 15.95 degree, at the 75% blade radius is 22 degree.

The chord length distribution along the radial direction is shown in Fig. 4.

It can be found from the Fig. 4 that maximum chord length is 0.15 m at the third profile, minimum chord length is 0.0363 m at the blade tip.

The lift coefficients, drag coefficients, attack angle along the radial direction are listed in Table 1.

The wooden fixed-pitched propeller designed by the present method is shown in Fig. 5.

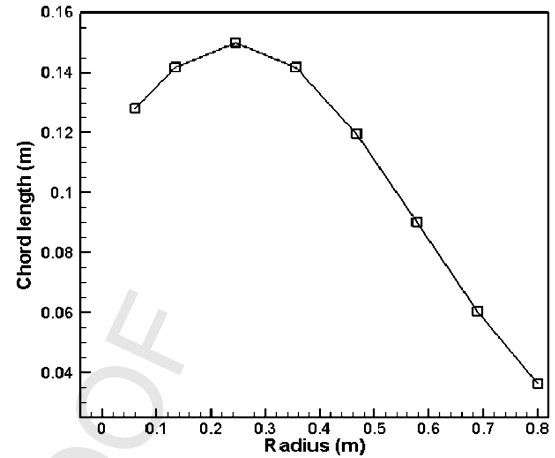


Fig. 4. The chord length distribution along the radial direction.

Table 1

The lift coefficients, drag coefficients, attack angle along the radial direction.

Radius (m)	Lift coefficient	Drag coefficients	Attack angle (degree)
0.0600	0.8351	0.0107	4
0.1340	0.8358	0.0097	4
0.2450	0.8394	0.0088	4
0.3560	0.7530	0.0075	3
0.4670	1.0550	0.0107	6
0.5780	0.7721	0.0078	3
0.6890	0.7841	0.0086	3
0.8000	0.7996	0.0099	3



Fig. 5. The propeller of an electric powered aircraft (diameter 1.6 m).

## 3. Wind-tunnel test of the scaled propeller

In order to verify the aerodynamic performance of propeller designed by the present method, wind-tunnel test of scaled propeller is carried out at the 3-D test section of NF-3 wind-tunnel of Northwestern Polytechnical University airfoil research center. The test section is the corner cut rectangular with width 3.5 m, height 2.5 m, length 12 m. Turbulence is 0.078% (see Fig. 6).

Diameter of scaled propeller is 0.96 m. Scaled propeller is shown in Fig. 7.

The scaled propeller installed on the wind-tunnel is shown in Fig. 8.

Wind speed  $V = 0$  m/s, 20 m/s, 30 m/s and 40 m/s. Rotation speed  $N = 900, 1200, 1500, 1800, 2100, 2400, 2700, 3000, 3300, 3600, 3900$  r/min.

Advanced ratio, thrust coefficient, torque coefficient, power coefficient, efficiency can be obtained by the Eqs. (13)–(17), respectively.

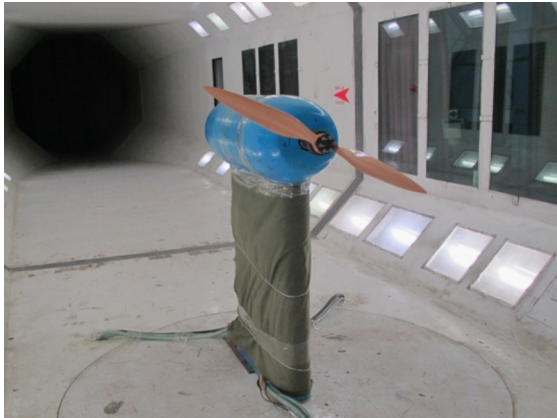
$$\lambda = \frac{V}{n_s D} \quad (13)$$

$$C_T = \frac{T}{\rho n_s^2 D^4} \quad (14)$$





Fig. 6. The 3-D test section of NF-3 wind-tunnel.

Fig. 7. Scaled propeller with diameter  $D = 0.96$  m.Fig. 8. Scaled propeller with diameter  $D = 0.96$  m.

$$C_Q = \frac{Q}{\rho n_s^2 D^5} \quad (15)$$

$$C_W = \frac{W}{\rho n_s^3 D^5} \quad (16)$$

$$\eta = \frac{C_T \lambda}{C_W} \quad (17)$$

where  $n_s$  is the rotation frequency,  $n_s = N/60$ ,  $D$  is propeller diameter,  $Q$  is torque,  $W$  is power,  $C_T$  is thrust coefficient,  $C_Q$  is torque coefficient,  $C_W$  is power coefficient,  $\eta$  is efficiency.

The MRF model method is a steady state approximation. The fluid in the rotor blade region is modeled as a rotating frame and the surrounding fluid is modeled in a stationary frame. The MRF model includes the geometry of the rotor blades. MRF method allows individual zones to rotate or translate. This is realized by dividing the problem domain into separate zones where the flow is solved in stationary or rotating coordinate systems. When the air flow is uniform, this method is very accurate. The MRF transforms the fluid velocities from stationary to rotating frames using the following equation:

Stationary Frame

$$\frac{\partial \rho \vec{V}}{\partial t} + \nabla \cdot (\rho \vec{V} \vec{V}) = -\nabla p + \nabla \cdot \tau + S \quad (18)$$

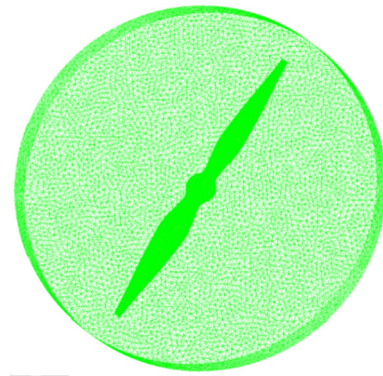


Fig. 9. The mesh of the rotor blade and rotor disc.

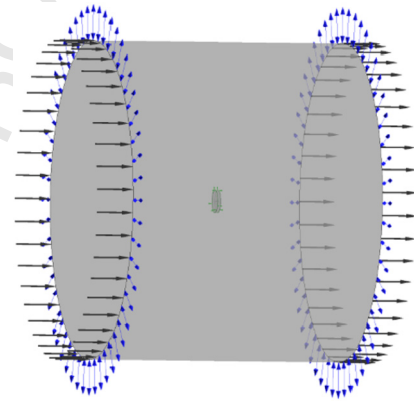


Fig. 10. Computational domain.

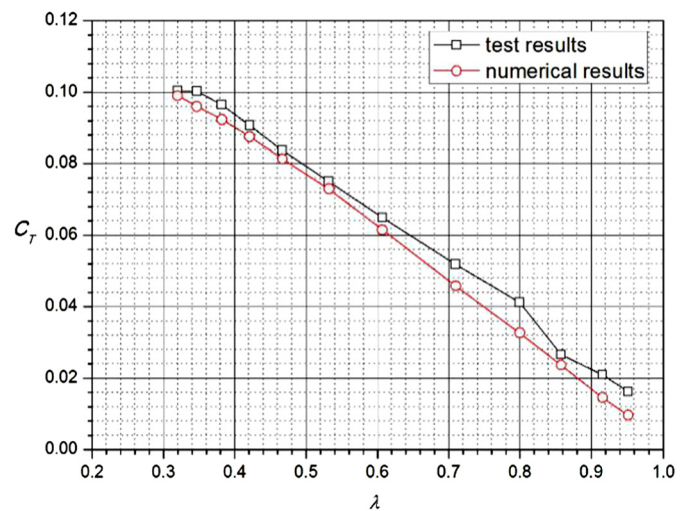


Fig. 11. Comparison of numerical results and test results of thrust coefficient.

$$\frac{\partial \rho \vec{V}_r}{\partial t} + \nabla \cdot (\rho \vec{V}_r \vec{V}_r) = -\rho (2\vec{\Omega} \times \vec{V}_r + \vec{\Omega} \times \vec{\Omega} \times \vec{r}) - \nabla p + \nabla \cdot \tau + S \quad (19)$$

MRF method solves the motion equations in the stationary and rotating frame. Therefore, with the general MRF capability, steady state analysis can be performed on various components of the rotating system using local reference frames, either stationary or rotating as appropriate. The mesh of the rotor blade and rotor disc is shown in Fig. 9. Computational domain is shown in Fig. 10.

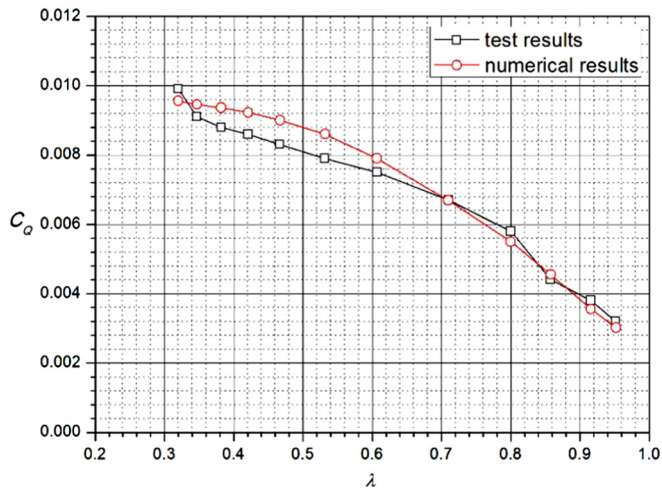


Fig. 12. Comparison of numerical results and test results of torque coefficient.

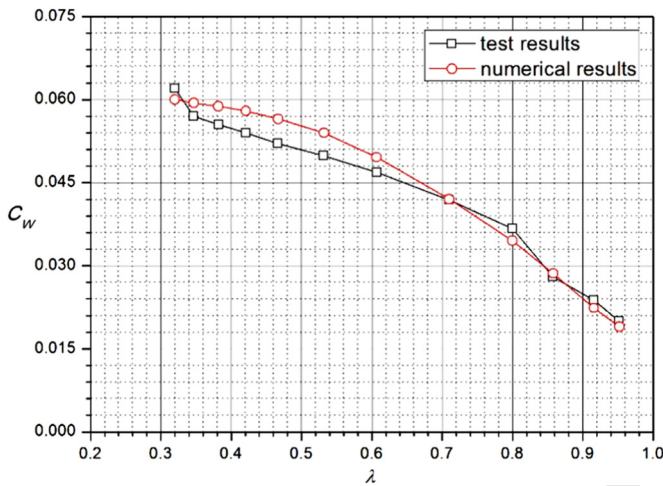


Fig. 13. Comparison of numerical results and test results of power coefficient.

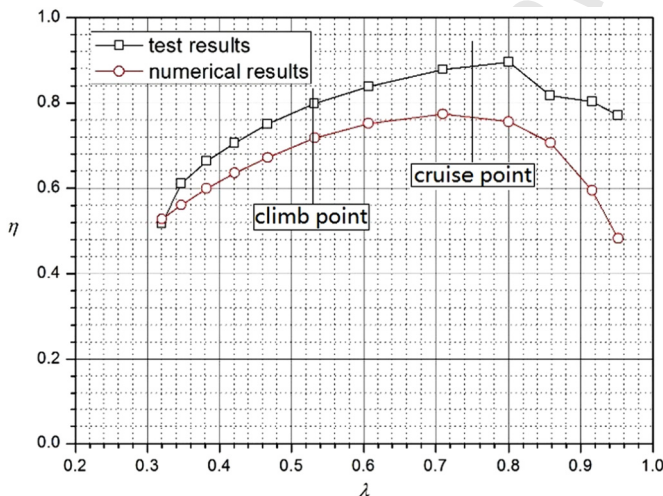


Fig. 14. Comparison of numerical results and test results of efficiency.

Comparison of numerical results and test results of thrust coefficient, torque coefficient, power coefficient and efficiency are shown in Figs. 11–14.

According to the Figs. 11–14, it can be found that numerical results of thrust coefficient, torque coefficient, power coefficient and

Table 2

The comparison of test results and numerical results for propeller efficiency.

$\lambda$	$\eta_{test}$	$\eta_{numerical}$	Error %
0.915	0.7573	0.6465	14.2%
0.8	0.8337	0.7530	9.6%
0.71	0.8354	0.7554	9.6%
0.638	0.8035	0.7354	8.5%
0.578	0.7722	0.7077	8.4%
0.528	0.7379	0.6772	8.3%
0.486	0.6990	0.6463	7.5%

efficiency are in good agreement with the wind-test results. The comparison of test results and numerical results for propeller efficiency is listed in Table 2.

#### 4. Conclusions

This paper presented an improved design method for propeller of an electric aircraft. According to the flight velocity, thrust and rotate speed of cruise condition, the propeller of an electric aircraft was designed using the present method. Wind tunnel test of scaled model of propeller (diameter 0.96 m) was carried out. The results show that numerical results of thrust coefficient, torque coefficient, power coefficient and efficiency are in good agreement with the wind-test results. The present method was suitable to design the propeller of the electric aircraft.

#### Conflict of interest statement

None declared.

#### Acknowledgements

This research was financially supported by research project of education department of Liaoning province (L201622), research project of Shenyang science and technology bureau (F16-205-1-07).

#### References

- [1] T. Tomažič, V. Plevnik, G. Veble, J. Tomažič, F. Popit, S. Kolar, R. Kikelj, J.W. Langelaan, K. Miles, Pipistrel Taurus G4: on creation and evolution of the Winning Aeroplane of NASA Green Flight Challenge 2011, *J. Mech. Eng.* 57 (12) (2011) 869–878.
- [2] G. Romeo, I.F. Borrello, E. Cestino, et al., ENFICA-FC: environmental friendly inter-city aircraft and 2-seat aircraft powered by fuel cells electric propulsion, in: *Airtech 2nd International Conference, "Supply on Wing"*, Frankfurt/Main, Germany, 2005.
- [3] G. Romeo, I. Moraglio, C. Novarese, ENFICA-FC: preliminary survey & design of 2-seat aircraft powered by fuel cells electric propulsion, in: *7th AIAA Aviation Technology Integration and Operation Conference, ATIO*, Belfast, Northern Ireland, 2007.
- [4] G. Romeo, F. Borello, ENFICA-FC: environmental friendly inter-city aircraft design and realization of 2-seater aircraft powered by fuel cells electric propulsion, in: *XX Associazione Italiana di Aeronautica e Astronautica Congress*, Milano, Italy, 2009.
- [5] G. Romeo, E. Cestino, F. Borello, et al., Engineering method for air-cooling design of two-seat propeller-driven aircraft powered by fuel cells, *J. Aerosp. Eng.* 24 (1) (2011) 79–88.
- [6] S.D. Angelo, F. Berardi, E. Minisci, Aerodynamic performances of propellers with parametric considerations on the optimal design, *Aeronaut. J.* 106 (1060) (2002) 313–320.
- [7] G. Romeo, E. Cestino, M. Pacino, F. Borello, G. Correa, Design and testing of a propeller for a two-seater aircraft powered by fuel cells, *J. Aerosp. Eng.* 226 (2012) 804–816.
- [8] S. Slavík, Preliminary determination of propeller aerodynamic characteristics for small aeroplanes, *Acta Polytech.* 44 (2) (2004) 103–108.
- [9] M. Sabzehparvar, In-flight thrust measurements of propeller-driven airplanes, *J. Aircr.* 42 (6) (2005) 1543–1547.
- [10] J. Morgado, M. Abdollahzadeh, M.A.R. Silvestre, J.C. Páscoa, High altitude propeller design and analysis, *Aerosp. Sci. Technol.* 45 (2015) 398–407.
- [11] J.A. Lieser, D. Lohmann, C.H. Rohardt, Aeroacoustic design of a 6-bladed propeller, *Aerosp. Sci. Technol.* 1 (6) (1997) 381–389.

- [12] M.H. Rizk, W.H. Jouj, Propeller design by optimization, *AIAA J.* 24 (9) (1986) 1554–1556.
- [13] J. Dorfling, K. Rokhsaz, Constrained and unconstrained propeller blade optimization, *J. Aircr.* 52 (4) (2015) 1179–1188.
- [14] L.K. Chang, J.P. Sullivan, Optimization of propeller blade twist by an analytical method, *AIAA J.* 22 (2) (1984) 252–255.
- [15] Y.X. Chen, P.Q. Liu, Z.H. Tang, H. Guo, Wind tunnel tests of stratospheric airship counter rotating propellers, *Theor. Appl. Mech. Lett.* 5 (2015) 58–61.